JOURNAL OF APPLIED ELECTROCHEMISTRY 8 (1978) 135–143

Ruthenium dioxide-based film electrodes. III. Effect of chemical composition and surface morphology on oxygen evolution in acid solutions[*]

G. LODI[†], E. SIVIERI, A. DE BATTISTI[†], S. TRASATTI

Laboratory of Electrochemistry, the University, Via Venezian 21, 20133 Milano, Italy

Received 30 May 1977

Oxygen evolution from acid solutions has been investigated on two kinds of RuO_2-based electrodes; compact and cracked (porous) films. The kinetic study has been carried out by means of potentiostatic curves. A method is suggested to estimate the surface concentration of active sites. The reaction order with respect to active sites and the activation energy have been determined. The mechanism is shown to differ on the two kinds of film in relation to the *S*(site)–OH bond strength and the surface concentration of intermediates. The behaviour of films on silica glass substrates is reported for the first time.

1. Introduction

RuO_2-based film electrodes prepared by the thermal decomposition of $RuCl_3 \cdot nH_2O$ on inert substrates are especially known for their use as anodes in chlor-alkali cells [1, 2]. The interest in their electrocatalytic properties, however, is not restricted to the chlorine evolution reaction. In a preliminary note from this laboratory [3] the oxygen evolution overvoltage on such electrodes has been reported to be one of the lowest ever observed. However, oxygen evolution on RuO_2-based electrodes has been sparsely studied [4–6] and mainly in alkaline solutions. Moreover, the relationship between the electrocatalytic properties and chemical composition of films has never been investigated explicitly. It has been shown [3, 7, 8] that the chemical composition closely depends on the temperature of preparation of films. The purpose of this work has been to investigate oxygen evolution from acidic solutions with special attention paid to the chemical composition and the morphology of films.

2. Experimental

2.1. *Electrodes*

The results reported in this work refer to three sets of electrodes prepared by different operators at different times. Two of these sets were prepared by the technique described elsewhere [7, 8]. Ti plates were first sand-blasted and then etched in hot 20% HCl, washed and rinsed in triply distilled water. A portion of approximately 0·1 M $RuCl_3$ solution in 20% HCl was dried by gentle heating and the residue was dissolved in the minimum amount of isopropanol. The required amount of substance was deposited onto the support by brushing. Few layers were necessary to complete the deposition. After each layer the solvent was eliminated at low temperature (*T*), then the electrode was fired at the selected *T* for 5 to 10 min. The films were finally annealed at the given *T* for one hour. The two sets of electrodes differed essentially because two ovens were used with differing air circulation efficiencies. In addition, the concentration of the starting solution

---

[*] Presented at the Euchem Conference on the Electrochemistry and Chemistry of Solids, 8–12 May 1977, Strasbourg (Le Howald), France. Part of this paper was first presented at the XI National Congress of the Italian Association of Physical Chemistry, 9–11 December 1976, S. Margherita Ligure, Italy.

[†] Present address: University of Ferrara, Ferrara, Italy.

in isopropanol may have been different, and also the brushing technique. Further, different firing times were adopted within the limits indicated above.

The third set was prepared by the procedure suggested by Lodi *et al.* [9]. The essential differences with respect to the other two sets were; (i) the oxygen circulation inside a quartz crucible where the electrodes were put before firing, (ii) longer firing *t* (15 min), (iii) two hours annealing, (iv) more dilute $RuCl_3$ solutions (2 wt.% in isopropanol, (v) dipping instead of brushing, and (vi) consequently a much higher number of layers needed to deposit the same amount of oxide (of the order of tens).

The optical difference between the two main groups of films is [9, 10] that the former is constituted presumably by porous layers with rough and cracked surfaces and the latter group consists of compact, relatively smooth and macro-porosity free layers. Measurements show [9] that the conductivity of the compact films is about three orders of magnitude higher than that [10] of the cracked films, and is comparable to that of stoichiometric RuO_2 crystals [11].

Compact electrodes were also prepared on silica glass. This support was chosen because there is evidence that the underlying metal may be anodically oxidized and may affect the stability of the oxide overlayer [12]. 1 × 1 cm glass plates provided with a thin glass stem were used. The stem was also covered with the oxide layer, then coppered electrolytically, soldered to a thin Cu wire and the soldering was finally coppered again electrolytically. It was then introduced into a small glass tube and fastened there with a suitable paste. The calculated thickness of the films was always 2 μm. With the purpose of enhancing the role of the surface area, a film was deposited on sintered glass. The available surface area was estimated *a posteriori* from voltammetric curves to be about two orders of magnitude higher.

The chemical composition of the films was determined by an X-ray energy dispersive micro-analyzer.

Films on silica glass may give rise to appreciable ohmic drops along the oxide layer to the glass stem. Measurements have shown* that the resistivity of the films exhibits a moderate inverse dependence on the firing *T* and may range from $1\text{–}3 \times 10^{-4}$ ohm cm. From the bottom of the electrode to the point from where the copper wire starts the resistance may range from 0·5 to 3 ohm depending on the length of the glass stem. Thus, when 2 mA flows the maximum ohmic drop along the entire electrode may range from 1 to 6 mV. Actually, the effective ohmic drop included in the potential measurements may be on average half the above values since the capillary coming from the reference electrode faces the centre of the electrode. Therefore, Tafel slopes can hardly be substantially affected by the ohmic drop in the films up to about 1 mA cm^{-2} in the worst case. Tafel slopes reported in this work have been measured as a rule at lower current densities.

2.2. *Procedure*

Oxygen evolution was carried out partly from 0·5 M H_2SO_4 and partly from 1 M $HClO_4$ solutions. No striking difference was observed as regards the effect of the nature of the electrolyte. Potentials were read with respect to a hydrogen electrode in the same solution (rhe). The potentiostatic technique was used to collect data. Electrodes were plunged into the solution and kept at 1·2 V for about 10 min. The potential was then increased by 10 mV steps and the current read after 30 s at each potential. Experiments were carried out at five temperatures between 20° C and 50° C. In some experiments, five curves at increasing *T* were determined in the same solution. In others, electrodes were kept outside the solution for at least 12 h between two experiments.

Triply distilled water was used to make solutions. No effect of degassing was observed. During experiments, solutions in the cell were stirred with a magnetic stirrer.

3. Results

Fig. 1 shows the relationship between the firing temperature of the films and the Ru and Cl content of the layers. No substantial difference in chemical composition apparently exists

---

* Detailed results will be reported in a forthcoming paper (part IV).

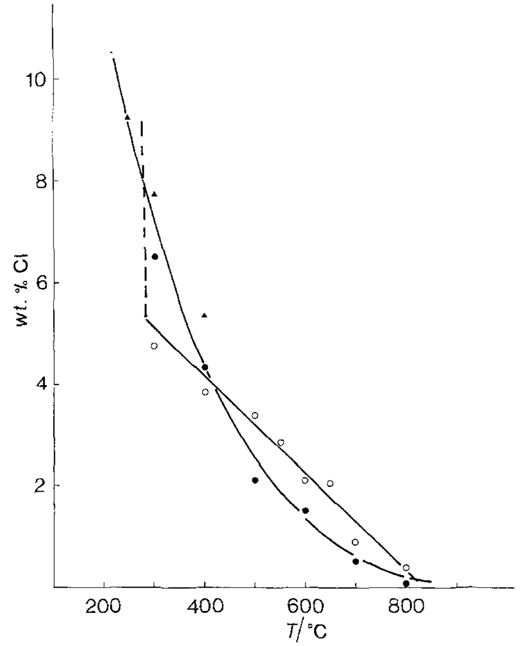

Fig. 1. Wt.% of Cl and Ru in RuO_2 from thermal decomposition of $RuCl_3$ as a function of firing *T*. (○) Powders [10]; (●) films on silica glass [9]; (▲) films on Ti.

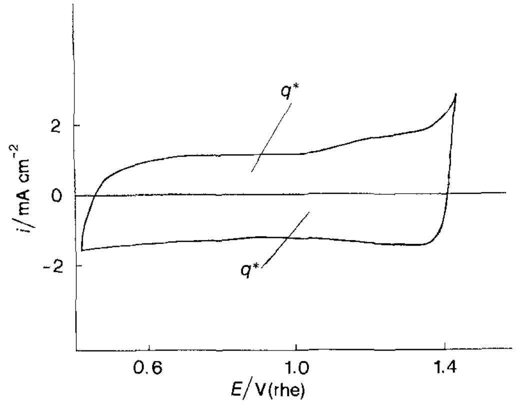

Fig. 3. Typical voltammetric curve at 50 mV s^{-1} for a RuO_2 film between 0·4 V and 1·4 V (rhe).

between cracked and smooth films, and powders (Pizzini *et al.* [10]).

Fig. 2 shows a typical Tafel plot for oxygen evolution on the RuO_2-based films. Curves on non-activated Pt and RuO_2 single crystals [3] are also reported for comparison. Higher overvoltages and Tafel slopes are always observed with stoichiometric RuO_2 as compared to films, which is an indication of substantially different mechanisms, although the roughness of the surface can have some effect on the actual value of the current density. This suggests that the origin of the catalytic properties of RuO_2 is not to be sought in the intrinsic structure of the dioxide. Also, suggestions [13] resting on a supposed [10] difference in the conductivity mechanism do not seem to be sound [14, 15]. Catalytic properties are more likely to originate from the state of surface atoms and thus oxygen evolution is expected to take place on catalytically active surface sites and not on all the available electrode surface.

The different chemical compositions of the films have been shown in previous papers to be measurable electrochemically by means of cyclic voltammetry [3, 7]. The principle of the method

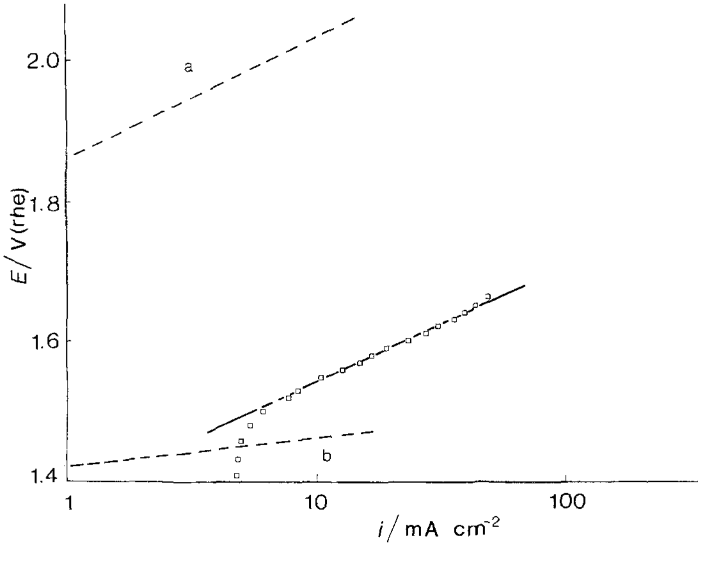

Fig. 2. Comparison of Tafel slopes for; (a) unactivated Pt, (b) RuO_2 films and (□) RuO_2 single crystals.

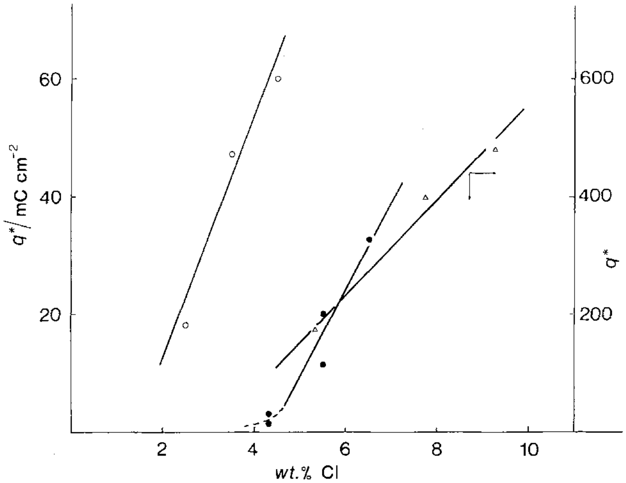

Fig. 4. Graphical correlation between charge as measured from voltammetric curves and Cl content of RuO_2 films for various sets of samples. (○, △) cracked films on Ti; (●) compact films on silica glass.

is illustrated in Fig. 3 which shows a voltammetric curve in acid solution between 0·4 and 1·4 V at 50 mV s^{-1}. Integrated anodic and cathodic charges are found to be approximately equal. Charges (q^*) have been found to depend on firing temperature, thickness, atmosphere of annealing, handling and heating rate. It was first pointed out elsewhere [3] that q^* may also be related to some residual hydration of the RuO_2 lattice.

Fig. 4 shows that within each group of electrodes a linear correlation exists between chlorine content and charge q^*. This corroborates the view that q^* is a measure of the chemical composition, but its actual value must depend on other factors too. Actually, optical inspection by scanning electron microscope (SEM) showed [9] that the roughness of the surface of compact films increased slightly with firing T, as should q^* were it merely proportional to the extent of the surface. The figure also shows that different sets of electrodes with the same Cl content may be characterized by different values of q^*. This effect is thought to be related to the morphology of films being extremely sensitive to details of the preparation procedure. The lower values of q^* for compact films are regarded as a piece of evidence for the smoothness and absence of macroporosity of the surface. It is thus possible to write

$$q^* = q_s^* + q_b^* \tag{1}$$

where q_s^* is the part of charge involved in surface transformations and q_b^* the charge associated with bulk effects.

Fig. 5 shows for compact films an attempt to separate the bulk and surface contributions to q^*. The constant value to which q^* tends as T is

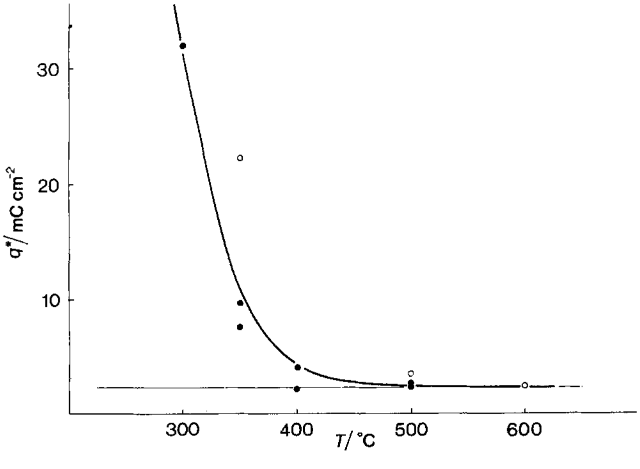

Fig. 5. Charge from voltammetric curves as a function of firing T. Compact films on Ti (●), and on silica glass (○).

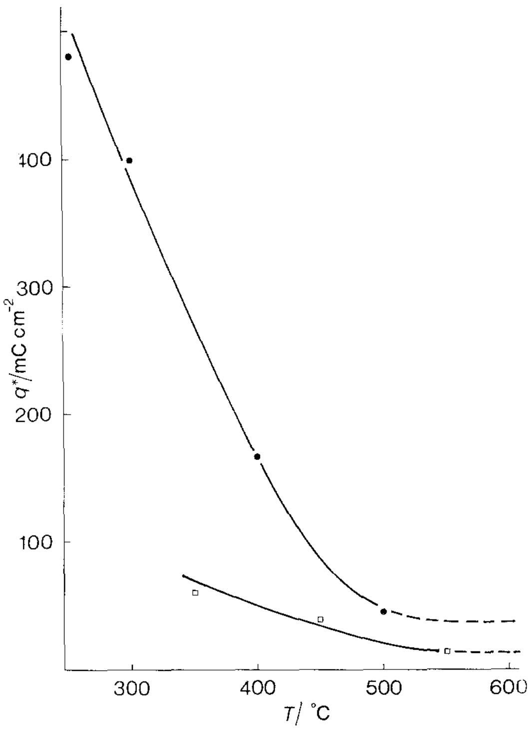

Fig. 6. Charge from voltammetric curves as a function of firing T for two sets of cracked films on Ti.

increased may be assumed, to a first approximation, to be associated only with surface modifications. q^* was found to level off at about 2 mC cm^{-2}. An approximate calculation [14] based on the structure of the (100) RuO_2 face [16] and including double layer charging suggests that the true to apparent surface area ratio may be about 8–20, the actual value depending on the exact nature of the surface modifications and of sites involved. Preliminary BET measurements showed that the roughness factor may be of the order of 10–20, in good agreement with the electrochemical data.

Fig. 6 shows the same plot as in Fig. 5 but for the two sets of cracked electrodes. Although available data are scarce in this case so that conclusions can only be tentative quantitatively, the group of films with lower q^* is estimated to have q_s^* about 7–10 times higher than that of the electrodes in Fig. 5, while the group with larger q^* presents a q_s^* 3–4 times higher still. This means that the true to apparent surface area ratio may be 60–200 for the group in the lower part of Fig. 6, and 20–800 for the other group. BET measurements for films [17] and for powders [10] made by other authors indicated that the roughness factor may be 200–250. Zn^{2+} adsorption suggested about 80 in another case [4]. These two values are not directly comparable because different adsorption sites may be involved, but the order of magnitude agrees with electrochemical data in this work for moderately cracked electrodes.

Fig. 7 shows typical Tafel lines for cracked and compact electrodes. The linearity is followed in an intermediate range of current. At lower i values the process is complicated by the intrinsic properties of the oxide layer, while at higher i values the deviation from linearity also observed by other authors [4–6] may be due to uncompensated ohmic drops and the diffusion of products, but possible modifications of electrode properties as the potential is made more anodic cannot be

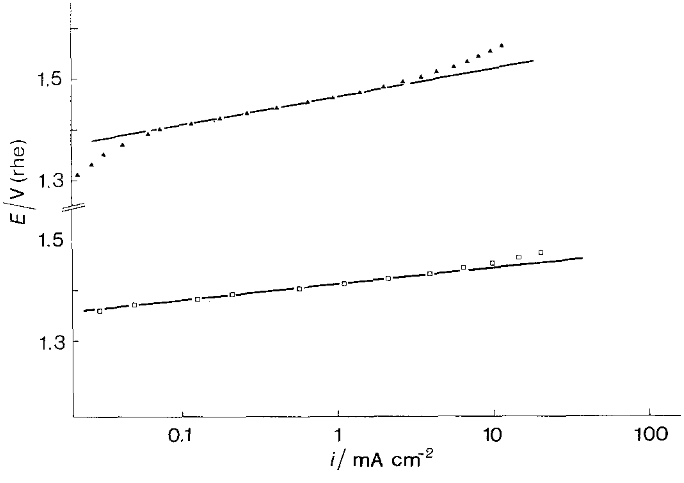

Fig. 7. Typical Tafel plots for two RuO_2 films, compact on silica glass (▲), and cracked on Ti (□).

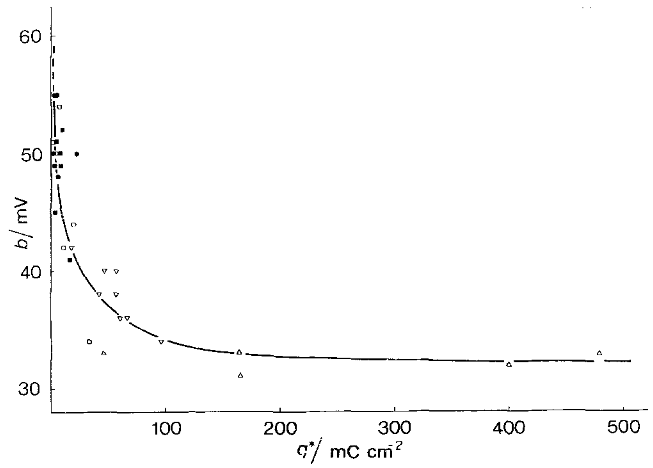

Fig. 8. Tafel slope as a function of charge from voltammetric curves. Symbols refer to different sets of electrodes. (○, ●) films on silica glass; all others on Ti. (△, ▽) cracked films.

ruled out. The latter view may be substantiated by the fact that the departure from linearity is observed at approximately the same potential, about 1·45 V. Pourbaix [18] suggests for the reaction

$$RuO_2 + H_2O \rightarrow RuO_4 + 4H^+ + 4e \qquad (2)$$

the value of 1·39 V for the standard potential.

Although the effect of pH has not been investigated in detail, the reaction rate at constant overvoltage can be recognized to be almost pH independent for cracked electrodes, whereas the slope of log i v. pH plots is close to 0·5 for compact electrodes and apparently decreases as q^* decreases.

Fig. 7 shows that Tafel slopes are higher for compact than for cracked films. This seems to be a general rule. Fig. 8 shows that there is a definite increase in the Tafel slope as q^* decreases. The plot in Fig. 8 shows some continuity between the various sets of electrodes. Cracked films are grouped in the range of 30 to 40 mV (b), while compact films exhibit Tafel slopes $\geqslant$ 40 mV.

A clear separation between compact and cracked films can be seen in Fig. 9 which shows Arrhenius plots at the potential of 1·4 V. Within each of the two groups electrodes exhibit the same activation energy, but this is higher for cracked than for compact films. Films on silica glass do not exhibit anomalous behaviour. The absolute value of $\Delta H^\dagger$ was found to depend on the experimental procedure, in the sense that the apparent $\Delta H^\dagger$ was higher if potentiostatic curves were made in one run at the various T's. Under strictly steady-state conditions, viz., if electrodes were left between two T's outside the solution for at least 12 h, the mean value of $\Delta H^\dagger$ was found to be about 12 kcal mol^{-1}. If account is taken of the observed decrease in $\Delta H^\dagger$ as the pH is increased,

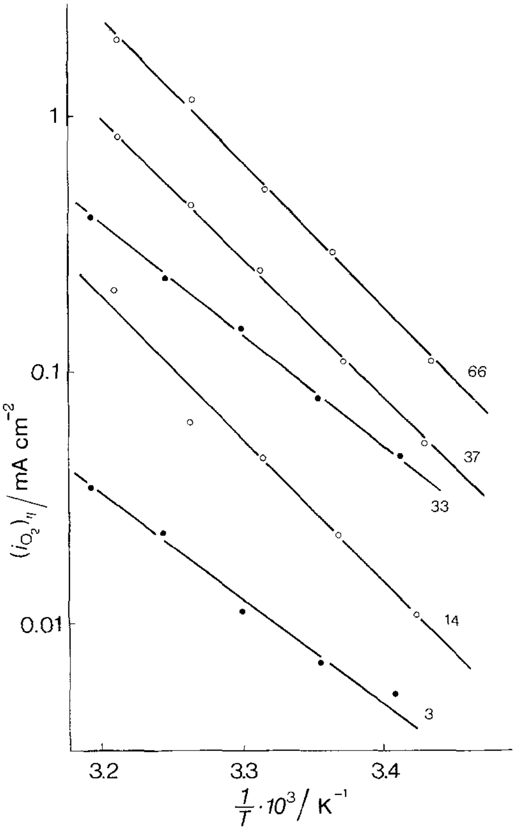

Fig. 9. Typical Arrhenius plots at 1·4 V (rhe). (○) Cracked and (●) compact films are distinguished. Charge q^* indicated by figures beside the lines.

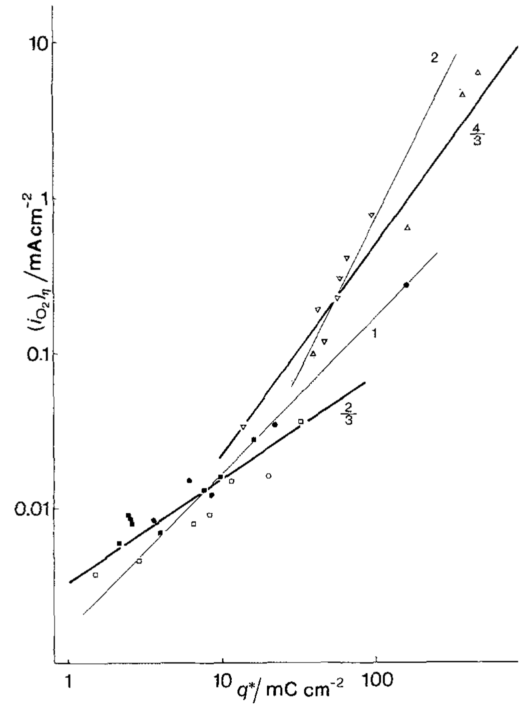

Fig. 10. Rate of oxygen evolution on RuO_2 films at 1·4 V (rhe) as a function of charge from voltammetric curves. Support: (□, ■, △, ▽) Ti; (○, ●) silica glass. Morphology: (△, ▽) Cracked and (□, ■, ○, ●) compact films. Solution: (□, ○) 0·5 M H_2SO_4; (△, ▽, ●, ■) 1 M $HClO_4$. Figures by the straight lines indicate the slope.

the value found in this work for acid solutions compares well with that of 9–10 kcal mol^{-1} obtained by other authors [5] in strongly alkaline solutions.

The most interesting aspect of the results is the dependence of the reaction rate of oxygen evolution at constant overvoltage on charge q^*. This does not seem to be a simple matter of surface area available for the reaction, in that the rate increases with decreasing firing T, quite the opposite of the findings with SEM suggesting that the profile of the surface becomes rougher as the firing T is increased. Since q^* has been shown to be essentially a measure of the morphology, the charge can be assumed to measure the surface concentration of active sites.

Fig. 10 shows a log–log plot of reaction rate at 1·4 V against q^*. It is interesting that the two groups of electrodes follow two different relationships. Smooth transition between the two groups cannot be recognized with certainty. Compact electrodes group around a straight line with slope ranging from 2/3 to 1. Cracked electrodes gather round a straight line with slope ranging from 4/3 to 2. The more probable value of the slopes is the lower one in both cases. These values are thought to indicate that the reaction order with respect to surface sites is 1 for compact films and 2 for cracked films. The lower value for the actual slope is attributed to the fact that according to Equation 1 q^* is a volume charge. In such a case the surface charge should be proportional to $q^{*2/3}$. Therefore, $(q^{*2/3})^2 = q^{*4/3}$ in the case of second order kinetics. It is interesting in this respect that the point for the sintered glass-supported electrode (closed circle at the extreme end of the group of compact electrodes in Fig. 10) fits better on the line of unit slope. In such a case q^* in fact measures mainly a surface charge.

4. Discussion

On the basis of the experimental results presented above, the following general scheme [19–21] is suggested for the mechanism of oxygen evolution on RuO_2-based film electrodes

$$S + H_2O \rightarrow S\text{–}OH + H^+ + e \qquad (3)$$

$$S\text{–}OH \rightarrow S\text{–}O + H^+ + e \qquad (4)$$

$$S\text{–}OH + S\text{–}OH \rightarrow S\text{–}O + S + H_2O \qquad (5)$$

$$S\text{–}O + S\text{–}O \rightarrow O_2 + 2S. \qquad (6)$$

S is an active surface site, whose nature depends on the defective structure of the film. It seems unlikely according to Fig. 2, that S might be a Ru^{4+} ion of the lattice in that stoichiometric RuO_2 exhibits higher overvoltages. S might be a higher valence Ru ion, but it is more likely to be a Ru ion in the defective region between small crystallites. According to this view, q^* would be a measure of the amount of proton penetration [3] into the bulk through preferential paths along micropores and grain boundaries. If this is the case, then q^* would measure the degree of crystallinity of the samples. This is expected to decrease as the firing T is lowered [9, 10, 22].

On stoichiometric single crystals the reaction of oxygen evolution is very likely to proceed with Equation 3 as the rate determining step (rds). On compact films, the most probable mechanism is via Steps 3, 4 and 6 with Equation 4 as the rds. The decrease in Tafel slope as q^* decreases may be taken to mean [23] that the *S*–OH bond strength decreases. Fig. 8 suggests tentatively that $b \rightarrow 0{\cdot}12$ V as $q^* \rightarrow 0$. The values of the Tafel slope indicate [20, 21] that the oxygen evolution takes place with very low surface concentration of intermediate species. An alternative possibility might be that as q^* decreases the rds does not change but turns smoothly to an activation-free condition [24]. If this were the case, then $b \rightarrow 0{\cdot}06$ V as $q^* \rightarrow 0$. However, other parameters [20] makes this possibility less probable. It may be suggested that a transition from a second electron transfer to a first electron transfer controlled mechanism (discharge) is the most probable occurrence. In this case at low q^* values a mixed kinetic path would be followed.

The above mechanism rules out the possibility that the *S*–OH bond strength increases as the chlorine content decreases as implied [20, 21] if the increase in *b* were associated with the same rds. However, it is possible that the increase in Tafel slope at high current densities is associated with an increase in the surface concentration of adsorbed OH species, although this is a very weak hypothesis in view of the instability of adsorbed oxygenated species on RuO_2 [16]. A further possibility is that at higher overvoltages sites on crystallites also start evolving oxygen with a higher Tafel slope.

On cracked electrodes, the most probable mechanism is via Steps 3, 5 and 6 with Step 5 as the rds. With respect to compact films, the *S*–OH bond strength should thus be increased. However, it is also possible that the reaction path may be related to enhanced surface diffusion due to macro- and microporosity of the layer which causes the reaction to proceed through Step 5 rather than Step 4. Actually, this happens even though the apparent activation energy is higher for the former than for the latter step.

It is interesting that Step 6 is always fast. In this respect, oxygen evolution can be regarded as a reaction of chemical decomposition of unstable higher Ru oxides. For instance

$$RuO_2 + H_2O \rightarrow RuO_3 + 2H^+ + 2e \qquad (7)$$

$$RuO_3 \rightarrow RuO_2 + O. \qquad (8)$$

RuO_3 is thermodynamically unstable [25, 26] and this is in agreement with the fact that the enthalpy of oxygen adsorption on RuO_2 was found [15] to be positive at as low coverages, θ, as 0·15, whereas it is high (130 kcal mol^{-1}) at $\theta \rightarrow 0$. The chemical view in Equations 7 and 8 is corroborated by the fact that oxygen evolution takes place in the potential range where, according to Equation 2, transition of RuO_2 to higher oxides is expected. Such a coincidence of potential ranges is not rare. It is for instance known [27], among others, for Co, Ag, Pd and Ni.

When this paper was ready to be submitted for publication, two papers by Tamura and co-workers [28, 29] appeared dealing with oxygen evolution from acid solutions on Ru and RuO_2, which are thought to corroborate strongly the conclusions reached in this work. Although the RuO_2 samples used by the above authors are in principle different from those used in this work because the former were derived from hydrous RuO_2 prepared by chemical precipitation, it is thought that their RuO_2 samples are similar to our weakly defective RuO_2 films. Conversely, non-protective oxide layers formed on Ru before oxygen evolution are thought to be comparable to our highly defective films. The mechanisms proposed by Tamura and co-workers are: chemical recombination on Ru, and electrochemical desorption on RuO_2, respectively. Further, the activation energy at 1·4 V (rhe) has been found to be higher on Ru (24·4 kcal mol^{-1}) than on RuO_2 (17·6 kcal mol^{-1}), and these values compare quite well to those found here at the same overvoltage (25 kcal mol^{-1} on cracked electrodes, and about 19 kcal mol^{-1} on compact films, respectively).

A definite conclusion which can be drawn from this work is that the electrocatalytic properties of RuO_2-based electrodes appear to be essentially related to the morphological structure of the surface rather than to chemical composition, although the two factors are to some extent interrelated.

Acknowledgements

The authors are indebted to Dr G. Buzzanca, Dr R. Rizzi and Dr D. Verri for help with experiments. Thanks are due to Dr. C. De Asmundis, Materials Chemistry, CNR, University of Genova, for chemical analysis of some of the films. Financial support by the CNR (Rome) is gratefully acknowledged.

References

[1] H. V. K. Udupa, R. Thangappan, B. R. Yadav and P. Subbiah, *Chem. Age India* **23** (1975) 545.

[2] R. R. Dukes and R. G. Milner, *J. Electrochem. Soc.* **117** (1970) 9C.

[3] S. Trasatti and G. Buzzanca, *J. Electroanal. Chem.* **29** (1971) A1.

[4] W. O'Grady, C. Iwakura, J. Huang and E. Yeager, 'Electrocatalysis', (Ed. M. W. Breiter), The Electrochemical Society, Princeton (1974) p. 286.

[5] G. Singh, M. H. Miles and S. Srinivasan, 'Nat. Bur. of Standards Special Publication 445', (Ed. A. D. Franklin) (1976) p. 289.

[6] E. Yeager, 'Nat. Bur. of Standards Special Publication 455', (Ed. A. D. Franklin) (1976) p. 203.

[7] D. Galizzioli, F. Tantardini and S. Trasatti, *J. Appl. Electrochem.* **4** (1974) 57.

[8] D. Galizzioli, F. Tantardini and S. Trasatti, *ibid* **5** (1975) 203.

[9] G. Lodi, C. Bighi and C. de Asmundis, *Mat. Sci.* **1** (1976) 177.

[10] S. Pizzini, G. Buzzanca, C. Mari, L. Rossi and S. Torchio, *Mat. Res. Bull.* **7** (1972) 449.

[11] W. D. Ryden and A. W. Lawson, *Phys. Rev.* **B1** (1970) 1494.

[12] T. Loucka, *J. Appl. Electrochem.* **7** (1977) 211.

[13] G. Bianchi, *ibid* **1** (1971) 231.

[14] S. Trasatti, *J. Electrochem. Soc.* **120** (1973) 1702.

[15] A. T. Kuhn and C. J. Mortimer, *ibid* **120** (1973) 1704.

[16] J. T. Sommerfeld and G. Parravano, *J. Phys. Chem.* **69** (1965) 102.

[17] A. T. Kuhn and C. J. Mortimer, *J. Electrochem. Soc.* **120** (1973) 231.

[18] M. Pourbaix, 'Atlas d'Equilibres Electrochimiques', Gauthier-Villars et G., Paris (1963).

[19] J. O'M. Bockris, 'Modern Aspects of Electrochemistry', (Ed. J. O'M. Bockris), Butterworth, London (1954) p. 180.

[20] B. E. Conway and M. Salomon, *Electrochim. Acta* **9** (1964) 1599.

[21] A. Damjanovic, 'Modern Aspects of Electrochemistry', (Eds. J. O'M. Bockris and B. E. Conway) 5, Butterworths, London (1969) p. 369.

[22] K. J. O'Leary and T. J. Navin, *Chlorine Bicent. Symp.* (1974) 174.

[23] P. Rüetschi and P. Delahay, *J. Chem. Phys.* **23**, (1955) 556.

[24] L. I. Krishtalik, *Elektrokhimiya* **4** (1968) 240.

[25] A. B. Nikolskij and A. N. Ryabov, *Zh. Neorg. Khim.* **10** (1965) 3.

[26] H. Schäfer, A. Tebben and W. Gerhardt, *Z. Anorg. Allg. Chem.* **321** (1963) 41.

[27] A. I. Krasilshchikov, *Zh. Fiz. Khim.* **37** (1963) 531.

[28] C. Iwakura, K. Hirao and H. Tamura, *Electrochim. Acta* **22** (1977) 335.

[29] C. Iwakura, K. Hirao and H. Tamura, *ibid* **22** (1977) 329.